

## CHAPTER 12

### RADIOMETER DESIGN CONSIDERATIONS

#### 12.1 *Components and Performance Characteristics*

The optics, detectors, and electronics are the basic elements of a radiometer. The optics collect the radiation, separate or disperse the spectral components, and focus the radiation to a field stop. The detectors, located behind the field stop, respond to the photons with a voltage signal. That voltage signal is amplified by the electronics and converted into digital counts.

Performance of a radiometer is characterized by its responsivity, detectivity, and calibration. The responsivity is a measure of the output per input. The detectivity is expressed as the ratio of the responsivity per noise voltage. Calibration attempts to reference the output to known inputs.

#### 12.2 *Spectral Separation*

The earth emitted radiation is detected in several spectral regions by radiometers where the spectral separation is accomplished by one of the following approaches. Band pass filters can be used to separate the infrared spectrum into parts of roughly 20 cm<sup>-1</sup>. Grating spectrometers and interferometers are capable of spectral resolution ( $\lambda / \Delta\lambda$ ) of about 1 / 1000. All three have been used to remote sense the earth.

#### 12.3 *Design Considerations*

##### 12.3.1 Diffraction

The mirror diameter defines the ability of the radiometer to resolve two point sources on the earth surface. The Rayleigh criterion indicates that the angle of separation,  $\theta$ , between two points just resolved (maxima of the diffraction pattern one point lies on the minima of the diffraction pattern of the other point)

$$\sin \theta = \lambda / d$$

where  $d$  is the diameter of the mirror and  $\lambda$  is the wavelength. The GOES satellite mirror diameter is 30 cm, so at infrared window wavelengths (10 microns) the resolution is about 1 km. This follows from

$$10^{-5} \text{ m} / 3 \times 10^{-1} \text{ m} = 3.3 \times 10^{-5} = r / 36,000 \text{ km}$$

or

$$r = 1 \text{ km} = \text{resolution.}$$

Diffraction is an important consideration when seeking clear FOVs in the vicinity of clouds. Clouds can affect measured radiances even when they are not directly in the FOV of the sensor. When clouds are close enough to the FOV, diffraction causes some of the radiation received by the sensor to emanate from the clouds instead of from the clear area within the FOV. As clouds are typically colder than the clear earth-atmosphere, measured radiances are lower than expected from a clear FOV. Sensors in geostationary orbit are usually diffraction limited because the FOV is small for the mirror diameter in order to achieve maximum spatial resolution. Thus when sounding with the geostationary sounders, the clear FOV must be sufficiently far away from cloud contamination to assure correct profile retrieval or a correction must be applied for cloud diffraction into the FOV.

Figure 12.1a shows the calculated diffraction effects for the new GOES imager for infrared window radiation in a clear scene of brightness temperature 300 K surrounded by clouds of 220, 260, or 280 K. The size of the clear scene is varied and the change in brightness temperature is plotted. These results use a FOV radius of 2 km, a mirror diameter of 31 cm, and a wavelength of 11 microns. Diffraction effects are noticeable for clear scenes as large as 50 km radius; for a cold cloud at 220 K, the brightness temperature of a 10 radius clear hole is too cold by about 1.5 K. Figure 12.1b shows the same plot for the GOES sounder infrared window with an 4 km radius FOV and the same optics; the diffraction effect is mitigated somewhat by the larger FOV of the sounder. Figure 12.1 indicates that to obtain clear sky brightness temperature within 1 K the clear area must be at least 15 km (10 km) in radius for the imager (sounder).

Diffraction is usually specified by encircled energy, the fraction of the total detected signal emanating from a circle of given size. For the GOES-8 imager infrared window this is given by 60% of the signal must come from a circle of one FOV diameter, 73% from 1.25 FOV diameter, and 79% from 1.5 FOV diameter.

### 12.3.2. The Impulse or Step Response Function

The detector collects the incident photons over a sampling time and accumulates a voltage response, which is filtered electronically. This is often characterized by the impulse (or step) response function, which details what the response of the sensor is to a delta (or step) function input signal. The response function is determined from the characteristics of the prealiasing filter which collects the voltage signal from the detector at the sampling times.

A perfect response of the detector continuously sampling a scene with a 100% contrast bar extending one FOV is indicated in Figure 12.2. As the detector crosses the contrast bar, the response ramps up linearly from 0 to 1 in the time it takes to move a distance of one FOV and then ramps down from 1 to 0 in a symmetric fashion. The actual response of the GOES-8 filter is also indicated in Figure 12.2. The shape a delay of the signal are noticeable. The filter delay causes an offset which can be corrected electronically. Sampling occurs every 183 microseconds or 1.75 times per FOV; the sampling interval is 4/7 of the time it takes to move one FOV.

Correcting for the time offset, the percentage of the total signal appearing in the samples preceding and following the correlated sample peak can be estimated. For GOES-8 infrared window samples one finds that sample N-2 has 4.3% of the total signal, N-1 has 26.5%, N peaks with 44.8%, N+1 has 23.4%, and N+2 has 1.0%. This causes a smearing of cloud edges and other radiance gradients.

Figure 12.3 shows the step response function for GOES-8. The filter output takes about 400 (or about 2 samples) microseconds to respond full scale to the step function input at time t=0.

### 12.3.3 Detector Signal to Noise

The noise equivalent radiance for an infrared detector can be expressed as

$$\text{NEDR}(\nu) = \gamma [\text{Ad } \Delta f]^{1/2} / [\text{Ao } \tau(\Delta\nu) \Omega \text{ D}^* \Delta\nu]$$

where

$\gamma$  is the preamplifier degradation factor which includes the effects of both preamplifier noise and signal loading

Ad is the detector area in cm<sup>2</sup>

$\Delta f$  is the effective electronic bandwidth of the radiometer

$A_o$  is the mirror aperture area in  $\text{cm}^2$

$\tau(\Delta\nu)$  is the transmission factor of the radiometer optics in the spectral interval  $\Delta\nu$

$\Omega$  is the solid angle of the FOV in steradians

$D^*$  is the specific spectral detectivity of the detector in the spectral band in  $\text{cm Hz}^{1/2} / \text{watt}$ , and

$\Delta\nu$  is the spectral bandwidth of the radiometer at wavenumber  $\nu$  in  $\text{cm}^{-1}$ .

Figure 12.4 indicates the spectral regions where the InSb and HgCdTe detectors show skill in detecting infrared radiation. The values of NEDR for the GOES-8 imager are indicated below.

Band	Wavelength (micron)	Detector	NEDR ( $\text{mW}/\text{m}^2/\text{ster}/\text{cm}^{-1}$ )	NEDT
1	.52 - .75	Silicon	(3 of 1023 counts is noise)	
2	3.83-4.03	InSb	0.0088	0.23 @ 300 K
3	6.5 - 7.0	HgCdTe	0.032	0.22 @ 230 K
4	10.2-11.2	HgCdTe	0.24	0.14 @ 300 K
5	11.5-12.5	HgCdTe	0.45	0.26 @ 300 K

#### 12.3.4 Infrared Calibration

The radiometer detectors are assumed to have linear response to infrared radiation, where the target output voltage is given by

$$V_t = \alpha R_t + V_o$$

and  $R_t$  is the target input radiance,  $\alpha$  is the radiometer responsivity, and  $V_o$  is the system offset voltage. The calibration consists of determining  $\alpha$  and  $V_o$ . This is accomplished by exposing the radiometer to two different external radiation targets of known radiance. A blackbody of known temperature and space (assumed to emit no measurable radiance) are often used as the two references. If  $z$  refers to space,  $bb$  the blackbody, the calibration can be written as

$$V_z = \alpha R_z + V_o$$

$$V_{bb} = \alpha R_{bb} + V_o$$

where

$$\alpha = [V_{bb} - V_z] / [R_{bb} - R_z]$$

and

$$V_o = [R_{bb} V_z - R_z V_{bb}] / [R_{bb} - R_z]$$

Using  $R_z=0$  this yields

$$R_t = R_{bb} [V_t - V_z] / [V_{bb} - V_z].$$

For HgCdTe detectors there sometimes is a non-linearity in the response to high photon bombardment occurring in the infrared window. In this case the IR calibration equation is given by,

$$R = q C^2 + m C + b$$

where

- R = calibrated scene radiance (dropping the t for target),
- C = digital counts (derived from the detector voltage with a linear analog to digital converter),
- q = second order gain (non-linear term),
- m = first order gain (slope), and
- b = count offset.

The second order gain is estimated before launch in vacuum tests as a function of radiometer temperature. The first order gain is obtained from the blackbody and space looks in flight (this occurs within every 20 minutes with GOES-8),

$$m = [R_{bb} - q (C_{bb}^2 - C_z^2)] / [C_{bb} - C_z]$$

and the count offset is updated after every space look (about every 2 minutes for GOES-8) using,

$$b = -m C_z - q C_z^2$$

where  $R_{bb}$  is calculated from blackbody thermistor data telemetered down from the spacecraft, and

$C_{bb}$  = digital counts during blackbody view, and

$C_z$  = digital counts during space view (before blackbody view).

The scan mirror of the radiometer telescope is usually not a perfect reflector, so there is some emission from the mirror that must be accounted for in the calibration algorithm. If the scan mirror emissivity is isotropic (independent of viewing angle), then its contributions to the target, blackbody, and space looks is constant and does not affect the calibration algorithm. However if the scan mirror emissivity changes with viewing angle, then the radiance detected must be written

$$R' = [1 - \epsilon(\theta)] R_t + \epsilon(\theta) R_m$$

where  $R_m$  denotes the mirror emitted radiance,  $R_t$  is the target radiance, and  $\epsilon(\theta)$  is the scan mirror emissivity at angle  $\theta$ . Then including the correction for the scan mirror emissivity variation, the first order gain is calculated after each blackbody view using,

$$m' = [R_{bb}' - q (C_{bb}^2 - C_z^2)] / [C_{bb} - C_z]$$

where

$$R_{bb}' = [1 - \epsilon(\theta_{bb})] R_{bb} + [\epsilon(\theta_{bb}) - \epsilon(\theta_z)] R_m$$

and

$\theta_{bb}$  = scan mirror angle while viewing the blackbody (incidence angle of bb radiation is about 45 degrees),

$\theta_z$  = scan mirror angle while viewing space (at about 40 and 50 degrees),

The offset is also adjusted through  $m'$

$$B' = -m' C_z - q C_z^2$$

The scan mirror emissivity corrected radiances are then calculated using,

$$R' = \{ q C^2 + m' C + b' - [\varepsilon(\theta_{bb}) - \varepsilon(\theta_z)] R_m \} / \{1 - \varepsilon(\theta)\}$$

Figure 12.5 shows the emissivity changes with angle and wavelength for the GOES-8 scan mirror. The radiance corrections,  $\Delta R = R' - R$ , for GOES-8 infrared window radiances are about 2 mW/m<sup>2</sup>/ster/cm-1 which convert to 1.2 C for a scene of 300 K.

The GOES-VAS satellites, which spin at 100 rpm, experience small diurnal temperature excursions. However, the GOES-8/9 satellites are three-axes stabilized so temperatures within the sensors vary by tens of degrees K over a 24 hour period. Therefore, the coefficients in the calibration equation must be updated frequently. To accomplish this, both the imager and the sounder view space routinely. The sounder views its blackbody every twenty minutes, while the imager normally views its blackbody every ten minutes unless doing so interrupts an image in process. At the most, the imager operates 30 minutes between blackbody views, e.g., when it makes a full-disk image. Drift in detector response (often referred to as 1/f noise (Bak *et al*, 1987)) dictates that the space and blackbody calibration looks occur frequently enough to keep changes in calibration within the specified noise levels. The ground system processing interpolates between calibration events, so that different calibration coefficients are determined for each data sample to account for the linear portion of the detector drift.

### 12.3.5 Bit Depth

The range of radiances expected for earth and atmosphere in a given spectral band must be converted to digital counts of fixed bit depth. This introduces truncation error. For n bit data, the radiance range, must be covered in 2<sup>n</sup> even increments. Consider the GOES-8 imager truncation errors indicated in the following table.

Band	$\lambda$ (micron)	Bit Depth	Rmax (mW/m <sup>2</sup> /ster/cm-1)	$\Delta R$	Tmax	$\Delta T(230)$ (degrees Kelvin)	$\Delta T(300)$
1	.65	10					
						(better detail in images)	
2	3.9	10	3.31	0.003	335	2.14	0.09
3	6.7	10	48.3	0.047	320	0.33	0.06
4	10.7	10	147.7	0.144	320	0.20	0.09
5	12.0	10	166.5	0.163	320	0.19	0.09

For earth scenes of 300 K, the truncation errors are small, less than a tenth of a degree Kelvin. However for cloud scenes of 230 K, the errors become greater than 2 K in the 3.9 micron band; this causes clouds to appear very noisy in this spectral band.

It is important that the truncation error is less than the error introduced by detector noise; this is true for GOES-8 since the NEDT at 300 K is about .2 C.

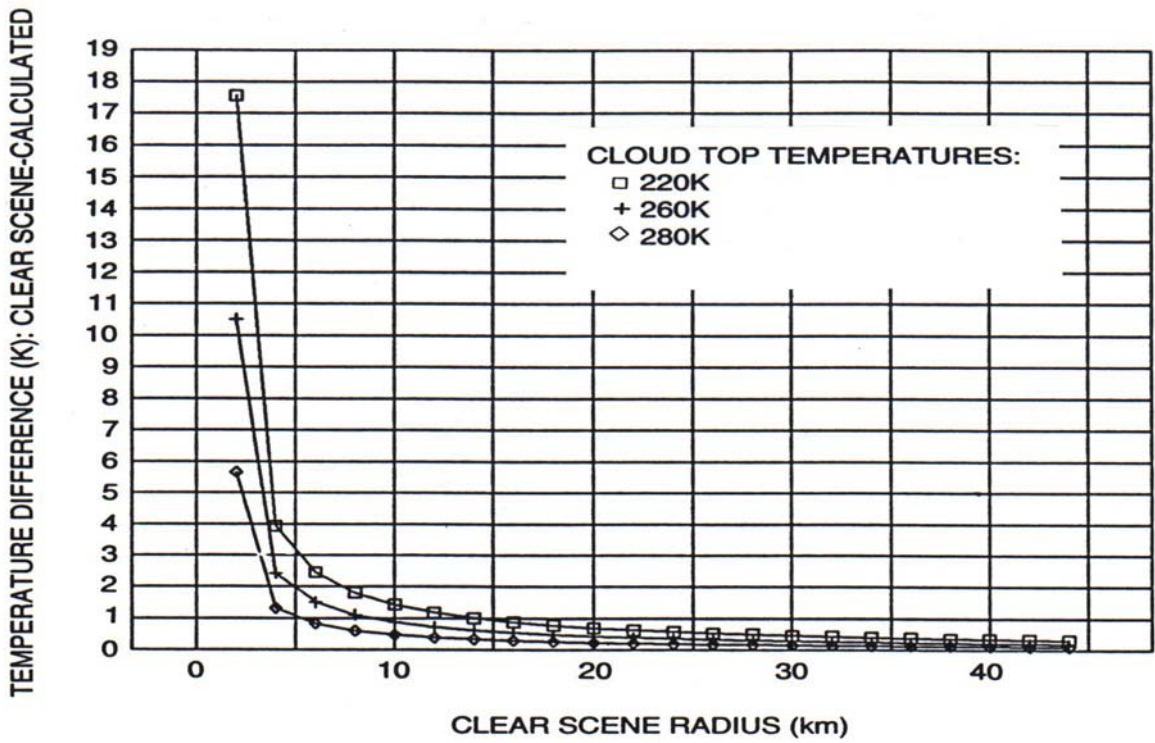


**Figure 12.1a:** Calculated diffraction effects for GOES imager infrared window radiation with a 2 km radius FOV in a clear scene of brightness temperature 300 K surrounded by clouds of 220, 260, or 280 K.

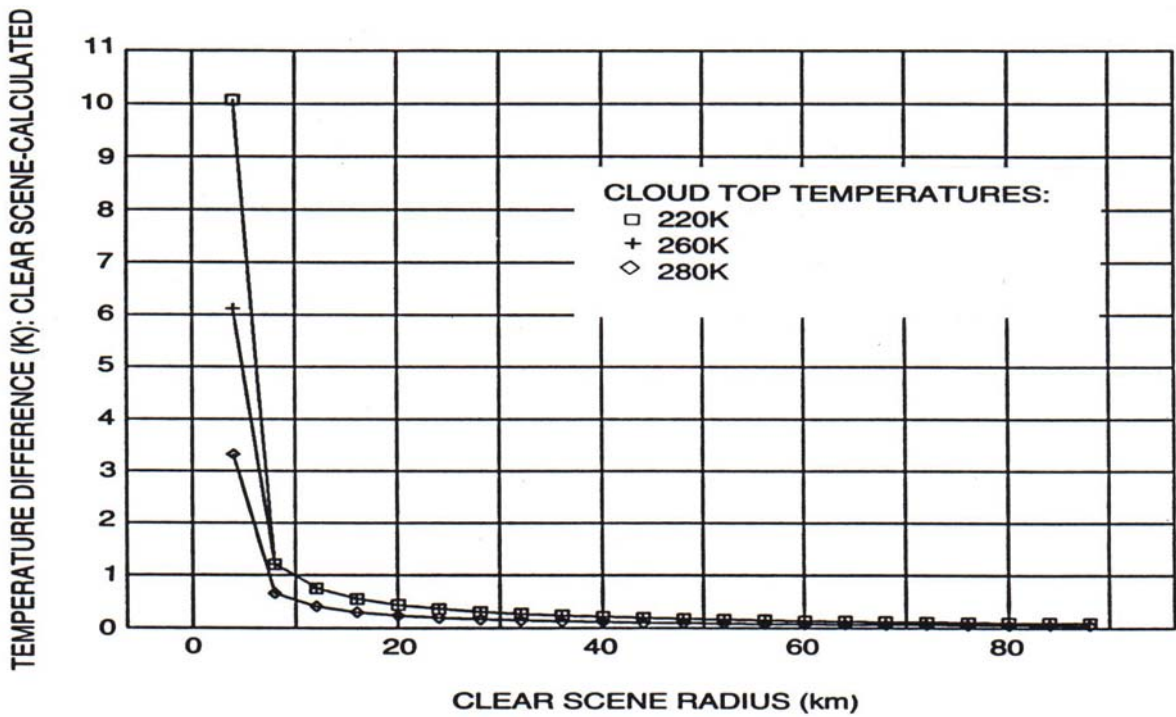


**Figure 12.1b:** Same plot for GOES sounder infrared window with a 4 km radius FOV and the same optics.

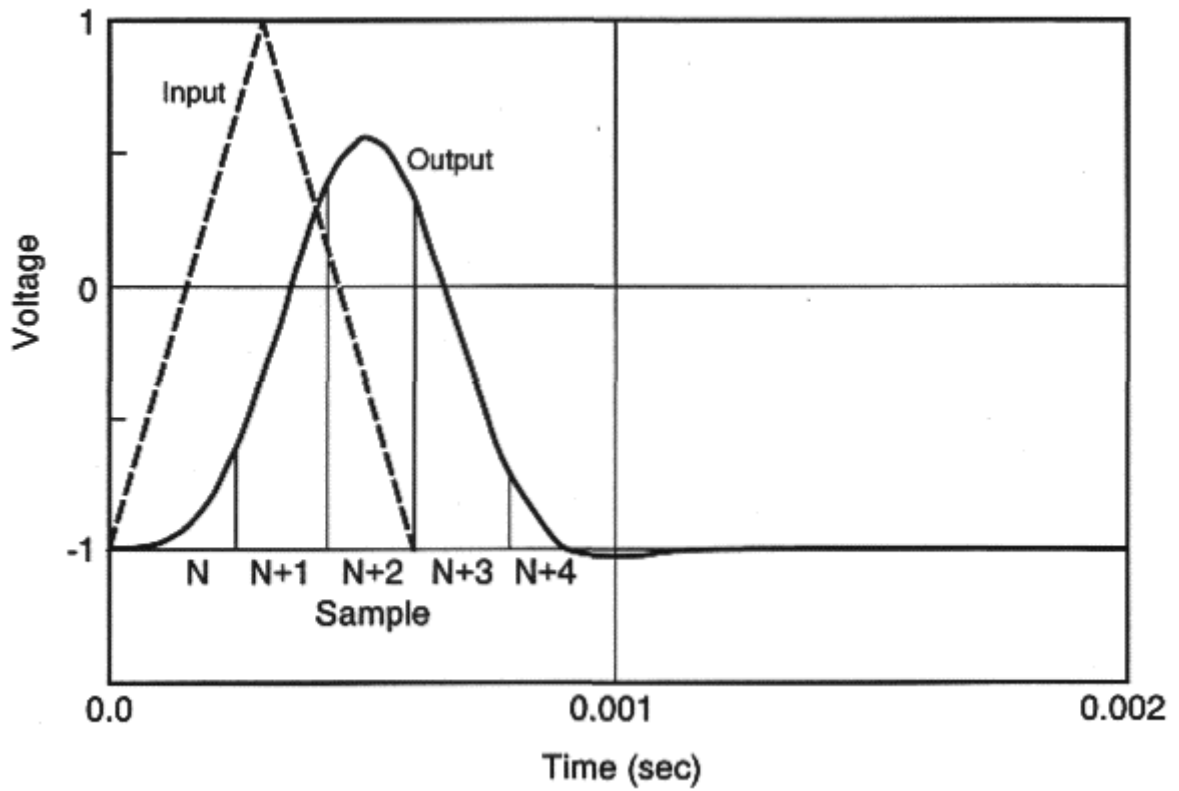


**Figure 12.2:** Perfect and actual response of the GOES-8 detector continuously sampling a scene with a 100% contrast bar extending one FOV.

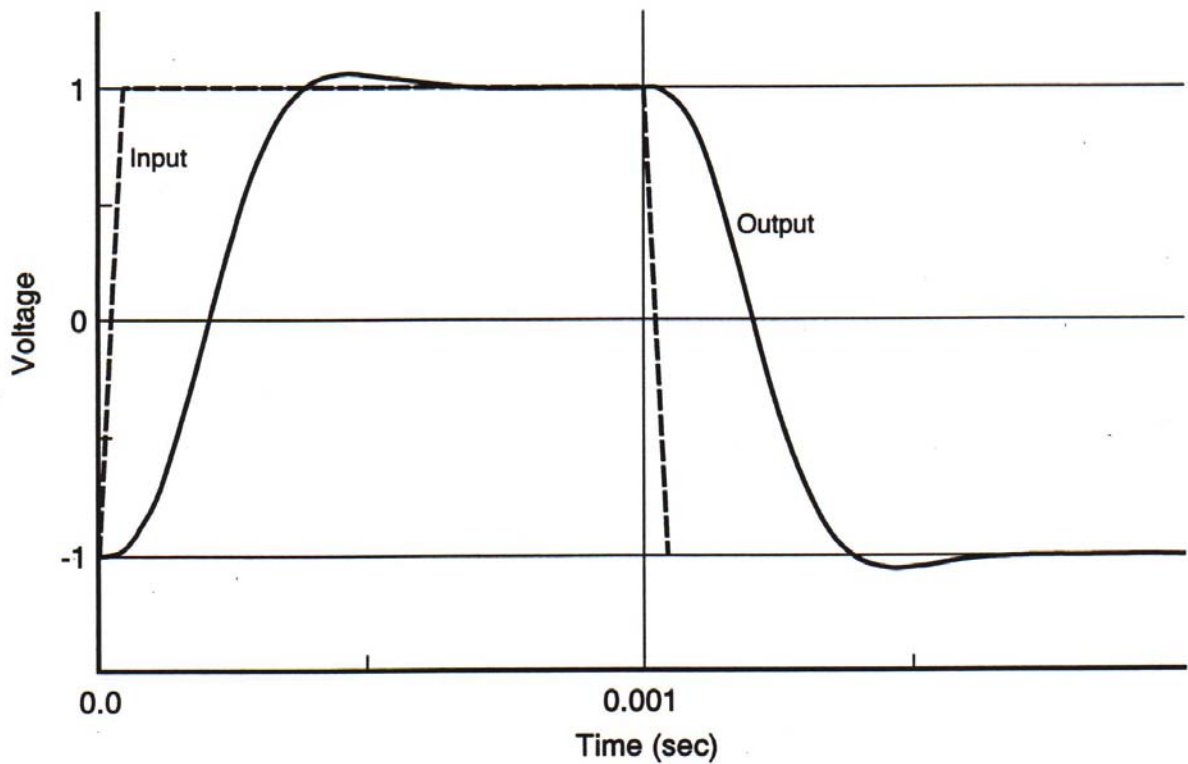


**Figure 12.3:** The step response function for GOES-8.

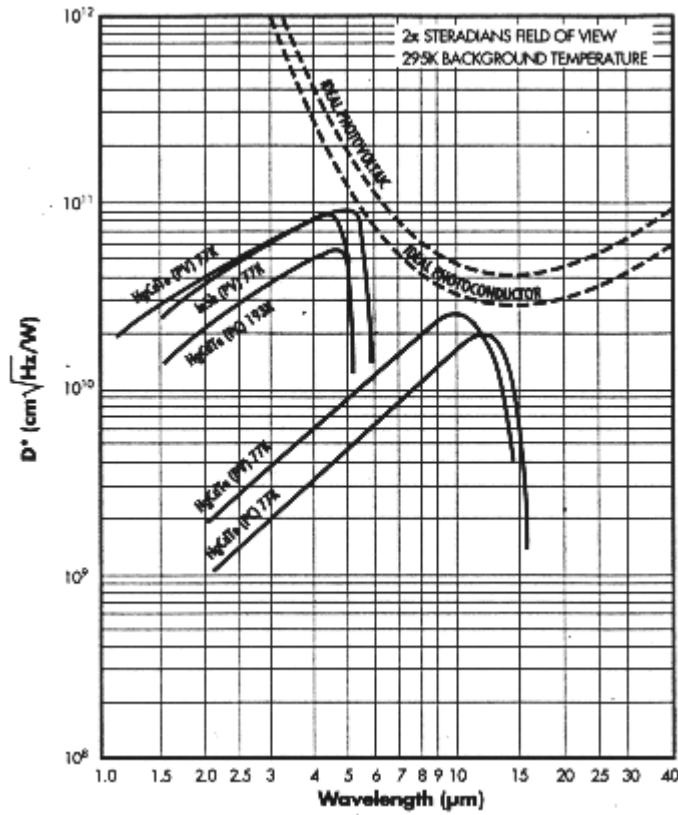


Figure 12.4: Detectivity of InSb and HgCdTe detectors as a function of spectral region.

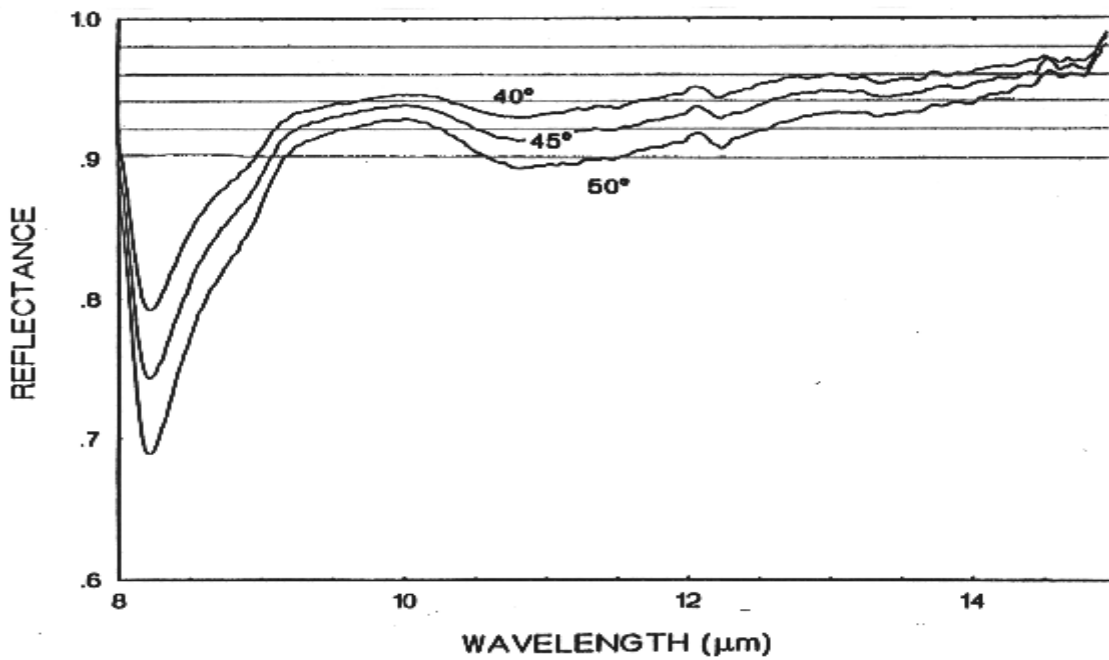


Figure 12.5: Emissivity changes with angle and wavelength for GOES-8 scan mirror.